Available online at www.sciencedirect.com
ScienceDirect
Chinese Journal of Aeronautics 20(2007) 481-487
Chinese Journal of Aeronautics
www.elsevier.com/locate/cja

Gain Scheduling Control of Nonlinear Shock Motion Based on Equilibrium Manifold Linearization Model

Cui Tao*, Yu Daren, Bao Wen, Yang Yongbin

College of Energy Science and Engineering, Harbin Institute of Technology, Harbin 150001, China

Received 28 November 2006; accepted 9 October 2007

Abstract

The equilibrium manifold linearization model of nonlinear shock motion is of higher accuracy and lower complexity over other models such as the small perturbation model and the piecewise-linear model. This paper analyzes the physical significance of the equilibrium manifold linearization model, and the self-feedback mechanism of shock motion is revealed. This helps to describe the stability and dynamics of shock motion. Based on the model, the paper puts forwards a gain scheduling control method for nonlinear shock motion. Simulation has shown the validity of the control scheme.

Keywords: shock motion; equilibrium manifold linearization; gain scheduling control

1 Introduction

Ramjet engine offers great potentialities to be as a propulsion system for supersonic guided missiles because of its simplified construction, low specific weight, and operational economy. The realization of the potential of this power plant is highly dependent upon the development of engine control systems capable of maintaining proper engine operation. A propulsion system control is, in general, required to perform two basic services: (1) to maintain desired engine performance throughout a flight plan, (2) to avoid unsteady operation. Because ramjet engine performance and security are directly related to the position of the normal shock within the inlet, normal shock position control has been investigated for decades.

In a ramjet inlet, supersonic flow is decelerated through a series of oblique shocks terminating with a quasi-normal shock at the position slightly downstream the inlet throat. The location of the normal shock directly influences the inlet efficiency and the peak performance will be obtained with the shock position rightly at the throat. However, the system with the shock position at the inlet throat or upstream inlet throat is unstable[1], which will result in expulsion of the shock system (inlet unstart)[2-4]. Moreover, disturbances originating in the freestream (e.g., turbulence) or in the subsonic portion of the inlet (e.g., at the compressor face) can cause the terminal shock momentarily to move into the upstream side of the throat, and thereby leads to inlet unstart. Inlet unstart, in turn, will induce a loss of propulsive efficiency and an asymmetric pressurization of the wing that would require large control surface forces to maintain aircraft control. The inlet tolerance can be improved by moving the normal shock farther downstream the inlet throat. However, this will increase the total pressure loss and might cause flow separation due to interaction between the stronger normal shock and the boundary layer.

*Corresponding author. Tel.: +86-451-86413241.
E-mail address: cuitao@hit.edu.cn
Foundation item: Hi-Tech Research and Development Program of China (2002AA723011)

Therefore, control of a terminal shock has a significant influence on supersonic inlet performance[5].

Various mathematical models used to design the normal shock control system have been studied. Since a complete mathematical description of the dynamic behaviors of normal shock is not only complex, but also highly nonlinear[6], model linearization becomes a common approximate method. Hurrell[7] used a linearizational method to investigate the effects of downstream pressure disturbances on the normal shock. A linearization model was developed by Willoh[8] to capture the shock motion, and another model by Culick[9] and Sajben[10] et al. to analyze the acoustic reflection and transmission properties of the normal shock. More recently, the linearizational model was extended by MacMartin[11] to represent the upstream and downstream perturbations as acoustic and entropy waves. A nonlinear model of shock wave trains in ducts with wall discontinuities was proposed by Alonso[12] to analyze the nonlinear process of shock motion. However, the nonlinear model can not be used as control model.

As from the previous studies, small perturbation methods have been applied for approximation and simplification. However, a small perturbation model is only effective when a system operates about a certain nominal operating position. To solve the problem, piecewise-linear methods are applied to enlarge the operating range, but a contradiction between accuracy and complexity happens in the use of the methods, which means too many models will be involved complexities in the control system design, and, moreover, a few of them will result in low accuracy. Another shortcoming is the discontinuous switching among different models, which may decreases the stability of the control system. With this consideration, Yu[13] developed an equilibrium manifold linearization model for nonlinear shock motion, which can achieve continuous global linearization with high accuracy and simplicity.

Based on the equilibrium manifold linearization model, this paper develops a gain scheduling control method for nonlinear shock motion.

2 Equilibrium Manifold Linearization

To begin with, a nonlinear plant is described by

$$\left.\begin{aligned}\dot{x}(t) &= f[x(t),u(t)]\\ y(t) &= h[x(t),u(t)]\end{aligned}\right\} \tag{1}$$

where f and h are smooth functions. The equilibrium manifold of the system described by Eq.(1) is a set defined as

$$\{(x,u)\mid f(x,u)=0\} \tag{2}$$

Assuming that the equilibrium manifold should be parameterized by a smooth function [$x(\alpha)$, $u(\alpha)$, $y(\alpha)$], where α is a scheduling variable, then

$$\left.\begin{aligned}f[x(\alpha),u(\alpha)] &= 0\\ h[x(\alpha)] &= y(\alpha)\end{aligned}\right\} \tag{3}$$

Linearizing Eq.(1) about its equilibrium manifold yields the parameterized linearization family[10]

$$\left.\begin{aligned}\frac{\mathrm{d}}{\mathrm{d}t}[x-x(\alpha)] &= A(\alpha)[x-x(\alpha)]+B(\alpha)[u-u(\alpha)]\\ y-y(\alpha) &= C(\alpha)[x-x(\alpha)]+D(\alpha)[u-u(\alpha)]\end{aligned}\right\} \tag{4}$$

where

$$\left.\begin{aligned}A(\alpha) &= \frac{\partial}{\partial x}f[x(\alpha),u(\alpha)]\\ B(\alpha) &= \frac{\partial}{\partial u}f[x(\alpha),u(\alpha)]\\ C(\alpha) &= \frac{\partial}{\partial x}h[x(\alpha),u(\alpha)]\\ D(\alpha) &= \frac{\partial}{\partial u}h[x(\alpha),u(\alpha)]\end{aligned}\right\} \tag{5}$$

3 Equilibrium Manifold Linearization for Modeling of Nonlinear Shock Motion

The nonlinear model of a normal shock can be expressed as

$$\frac{\mathrm{d}x_{\mathrm{s}}}{\mathrm{d}t} = F(x_{\mathrm{s}},J_2^-) \tag{6}$$

where x_{s} is the normal shock position, and J_2^- denotes the perturbation acoustic wave at downstream side of the normal shock, which can be described by

$$J_2^- = u_2 - \frac{2}{k-1}a_2 \tag{7}$$

where subscript "2" denotes the locations downstream of the normal shock.

According to Ref.[9], the unsteady shock motion can be expressed by

$$\frac{\mathrm{d}x_\mathrm{s}}{\mathrm{d}t}=\frac{[(k-3)u_1-(k+1)u_2]+\sqrt{16a_1{}^2+(k+1)^2(u_1-u_2)^2}}{4} \tag{8}$$

$$\frac{\mathrm{d}x_\mathrm{s}}{\mathrm{d}t}=\sqrt{\frac{(k^2-6k+1)a_1{}^2+(k+1)^2a_2{}^2+\sqrt{16k(k-1)^2a_1{}^4+[(k+1)^2a_2{}^2+(k^2-6k+1)a_1{}^2]^2}}{4k(k-1)}}-u_1 \tag{9}$$

Assuming that upstream conditions should be constant, the upstream variables u_1 and a_1 can be expressed as a function of x_s, while the downstream variables u_2 and a_2 as the perturbations. Eqs.(8)-(9) can be written into

$$\frac{\mathrm{d}x_\mathrm{s}}{\mathrm{d}t}=f_u(x_\mathrm{s},u_2) \tag{10}$$

$$\frac{\mathrm{d}x_\mathrm{s}}{\mathrm{d}t}=f_a(x_\mathrm{s},a_2) \tag{11}$$

where f_u and f_a represent the right-hand sides of Eqs.(8)-(9) respectively.

According to the equilibrium manifold linearization method, the equilibrium manifold of nonlinear shock motion is defined as

$$\left.\begin{aligned}(x_\mathrm{s}(\alpha),\ u_2(\alpha))\big|f_u(x_\mathrm{s}(\alpha),\ u_2(\alpha))=0\\(x_\mathrm{s}(\alpha),\ a_2(\alpha))\big|f_a(x_\mathrm{s}(\alpha),\ a_2(\alpha))=0\end{aligned}\right\} \tag{12}$$

The partial differential coefficients are calculated by

$$A_u(\alpha)=\frac{u_1[(k-1)Ma_1^2+2]}{2(1-Ma_1^4)}\frac{1}{A}\frac{\mathrm{d}A}{\mathrm{d}x} \tag{13}$$

$$B_u(\alpha)=-\frac{1}{4}\left((k+1)+\frac{(k+1)^2(u_1-u_2)}{\sqrt{16a_1{}^2+(k+1)^2(u_1-u_2)^2}}\right) \tag{14}$$

$$A_a(\alpha)=\frac{u_1[(k-1)Ma_1^2+2]^2}{4(1-Ma_1^2)(kMa_1^4+1)}\frac{1}{A}\frac{\mathrm{d}A}{\mathrm{d}x} \tag{15}$$

$$B_a(\alpha)=\frac{a_2\left((k+1)^2+\dfrac{(k+1)^2\left[a_2{}^2(k+1)^2+a_1{}^2(k^2-6k+1)\right]}{\sqrt{16k(k-1)^2a_1{}^4+[(k+1)^2a_2{}^2+(k^2-6k+1)a_1{}^2]^2}}\right)}{4\sqrt{k(k-1)}\sqrt{(k^2-6k+1)a_1{}^2+(k+1)^2a_2{}^2+\sqrt{16k(k-1)^2a_1{}^4+[(k+1)^2a_2{}^2+(k^2-6k+1)a_1{}^2]^2}}} \tag{16}$$

where A is the cross-sectional area, and subscript "1" denote the locations upstream of the normal shock.

After the equilibrium manifold and the partial differential coefficients have been calculated, the following final equations can be obtained:

$$\frac{\mathrm{d}}{\mathrm{d}t}[x_\mathrm{s}-x_\mathrm{s}(\alpha)]=A_u(\alpha)[x_\mathrm{s}-x_\mathrm{s}(\alpha)]+B_u(\alpha)[u_2-u_2(\alpha)] \tag{17}$$

$$\frac{\mathrm{d}}{\mathrm{d}t}[x_\mathrm{s}-x_\mathrm{s}(\alpha)]=A_a(\alpha)[x_\mathrm{s}-x_\mathrm{s}(\alpha)]+B_a(\alpha)[a_2-a_2(\alpha)] \tag{18}$$

The next step is to combine the perturbation variables of a_2 and u_2 into the acoustic perturbation wave J_2^-. According to the definition of J_2^-, the equilibrium manifold linearization model can be obtained as follows:

$$\frac{\mathrm{d}x_\mathrm{s}}{\mathrm{d}t}=\frac{(k-1)B_a(\alpha)A_u(\alpha)-2B_u(\alpha)A_a(\alpha)}{(k-1)B_a(\alpha)-2B_u(\alpha)}[x_\mathrm{s}-x_\mathrm{s}(\alpha)]+\frac{(k-1)B_a(\alpha)B_u(\alpha)}{(k-1)B_a(\alpha)-2B_u(\alpha)}\left\{u_2-\frac{2}{k-1}a_2-\left[u_2(\alpha)-\frac{2}{k-1}a_2(\alpha)\right]\right\}=\frac{(k-1)B_a(\alpha)A_u(\alpha)-2B_u(\alpha)A_a(\alpha)}{(k-1)B_a(\alpha)-2B_u(\alpha)}[x_\mathrm{s}-x_\mathrm{s}(\alpha)]+\frac{(k-1)B_a(\alpha)B_u(\alpha)}{(k-1)B_a(\alpha)-2B_u(\alpha)}\left[J_2^--J_2^-(\alpha)\right] \tag{19}$$

Parameterizing the equilibrium manifold by a scheduling variable α is an essential point of the method. The normal shock position x_s is defined as a scheduling variable:

$$\alpha=x_\mathrm{s} \tag{20}$$

Then, the equilibrium manifold linearization model can be written into

$$\frac{\mathrm{d}x_\mathrm{s}}{\mathrm{d}t}=T(x_\mathrm{s})\left[J_2^--J_2^-(x_\mathrm{s})\right] \tag{21}$$

$$T(x_\mathrm{s})=\frac{(k-1)B_a(x_\mathrm{s})B_u(x_\mathrm{s})}{(k-1)B_a(x_\mathrm{s})-2B_u(x_\mathrm{s})} \tag{22}$$

where $T(x_\mathrm{s})$ is the integral time constant.

4 Model Analysis

The following analysis is aimed at better un-

derstanding the connotative physical significance and application merits.

4.1 The self-feedback mechanism of shock motion

As discussed above, the equilibrium manifold linearization model can achieve the decoupling of the steady-state and dynamic behaviors of the nonlinear shock motion, where the steady-state behaviors are described by the equilibrium manifold $\{x_s, J_2^-(x_s)\}$, while the dynamic behaviors by the integral time constant $T(x_s)$.

Firstly, the steady-state behaviors of the nonlinear shock motion are analyzed. Formally, when the system is on the equilibrium manifold, J_2^- will be determined by the shock position x_s. However, if the shock is in a constant-area channel, J_2^- will be constant and independent of x_s. This means that the variable, which directly determines the value of J_2^-, is not the shock position x_s, but the cross-sectional area A. With this, the equilibrium manifold can be redefined as $\{A, J_2^-(A)\}$, where, $A=A(x_s)$. Although the redefinition may be useless in mathematics, it may be helpful to understand the physical mechanism of the shock motion.

Secondly, the dynamic behaviors of nonlinear shock motion are analyzed. From the view of control applications, the equilibrium manifold linearization model, described by Eq.(21), can be expressed as an integral process with a physical feedback shown in Fig.1. It indicates that the motion of a normal shock is a self-feedback system characterized by a self-balance or a dynamic imbalance.

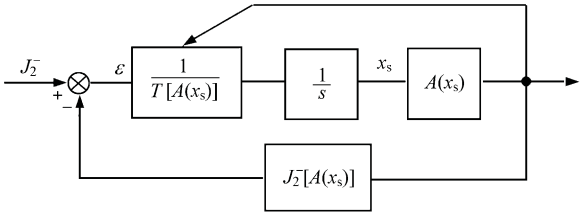

Fig.1 Equilibrium manifold linearization model.

To investigate the self-feedback mechanism of the nonlinear shock motion, a residual error ε is defined as

$$\varepsilon = J_2^- - J_2^-[A(x_s)] \tag{23}$$

where ε is also the perturbation which provides the driving force. If ε equals zero, the shock will be staying at a place.

For a given acoustic wave J_2^-, can be acquired

$$\frac{\mathrm{d}\varepsilon}{\mathrm{d}t} = -\frac{\mathrm{d}J_2^-[A(x_s)]}{\mathrm{d}t} = -\frac{\mathrm{d}J_2^-[A(x_s)]}{dx_s}\frac{\mathrm{d}x_s}{\mathrm{d}t} = -\frac{\mathrm{d}J_2^-[A(x_s)]}{\mathrm{d}x_s}\frac{1}{T[A(x_s)]}\varepsilon = \lambda\varepsilon \tag{24}$$

$$\lambda = -\frac{u_2[A(x_s)]}{1-Ma_2[A(x_s)]}\frac{1}{T[A(x_s)]}\frac{1}{A}\frac{\mathrm{d}A}{\mathrm{d}x} \tag{25}$$

where λ is the eigen value of the residual error equation for determining the stability of the self-feedback system. As is known, the system will be unstable when λ is positive, yet stable when negative. If λ equals zero, the system will be in a critical state. As shown in Eq.(25), the sign of λ is determined by $\mathrm{d}A/(A\mathrm{d}x)$, therefore, the stability of the self-feedback system is determined by the profile of the cross-sectional area.

The self-feedback mechanism of the shock motion can be described as follows: in a diverging channel, the self-feedback system is negative and the shock motion is stable due to the resistance from the negative feedback; in a converging channel, the self-feedback system is positive feedback, and the shock motion is unstable due to the propulsion from the positive feedback; while in a constant-area channel, the self-feedback system will change into a pure integral process with no feedback, which means that with the constant perturbation ε, the shock moves at a constant speed $\mathrm{d}x_s/\mathrm{d}t$, where the relation between ε and $\mathrm{d}x_s/\mathrm{d}t$ is determined by the integral time constant $T[A(x_s)]$.

4.2 The application merits of the equilibrium manifold linearization model

Next, as shown in Fig.1, for any given value of the scheduling variable x_s, the equilibrium manifold $J_2^-[A(x_s)]$ and the integral time constant $T[A(x_s)]$ can be automatically changed. In this way, a global linearization model is obtained with a good combination of high accuracy and low complexity. On the other hand, because the parameters of the model can be automatically scheduled by the scheduling variable x_s, there is no need for any switching to

other different small perturbation models, such as the piecewise-linear method, which may decrease the stability of the control system.

Another underlying merit of the equilibrium manifold linearization model worth pointing out is its further application in identifying the practical shock motion with test data. The actual supersonic inlet involves shock/turbulent boundary layer interaction, and the conclusions based on the theoretic model herein should be firstly considered as an initial guidance. Fortunately, the equilibrium manifold linearization method has an inimitable above-mentioned feature to achieve the decoupling of the steady-state and dynamic behaviors of the complex physical system. This is helpful in providing a simplified model configuration for identifications, in which the equilibrium manifold and the partial differential coefficients are the unknown functions of the scheduling variable x_s to be identified. In practical identifications, the equilibrium manifold can be identified by the steady-state test data, and then the partial differential coefficients should be identified by the dynamic test data.

5 Gain Scheduling Control Method

The work to design a linearization gain scheduled controller contains designing a linear controller family corresponding to the plant linearization family. The results in a linear controller family are parametrized by the scheduling variable α. These are local deviation signals associated with the linearized plant near the equilibrium parametrized by α. With this consideration, there is a natural link between the gain scheduling control and the equilibrium manifold linearization model.

Fig.2 shows the control system of shock motion including the perturbation waves, shock dynamics, actuator and controller. The actuator is a fuel-supplied system whose time constant is L. $\widetilde{x}_s$ is a designated value, d the disturbance signal, U the control variable which drives the fuel-supplied system, and M is the fuel flow rate.

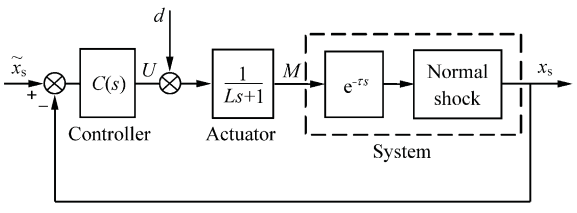

Fig.2 Control system of shock motion.

5.1 Control shortcomings

Controlling shock motion is to keep the shock at a designated position $\widetilde{x}_s$. Therefore, the main task is to compensate for disturbances. The control shortcomings are: (1) steady error $C_\infty = 0$; (2) peak value error of unit step disturbance $C_m < 20\%$; (3) phase reserve $\gamma_c > 50°$.

5.2 Control arithmetic

Gain scheduling control is an effective way of controlling systems whose dynamics changes with the operating conditions. It is normally used in the control of nonlinear plants, in which the relationship between the plant dynamics and operating conditions is known, and for which a single linear time-independent model is sufficient. A gain scheduling control system can be viewed as a feedback control system in which the feedback gains are adjusted using feedforward compensation. The typical design procedure of gain scheduling control involves the following steps: (1) selection of scheduling variable α; (2) construction of linear-invariant approximation to the plant at the ith operating point; (3) design of linear controller at each operating point; (4) design of gain scheduling scheme.

As for the problem of regulation, PID regulation is the commonly used method. Fig.3 shows the PID regulation system of shock motion.

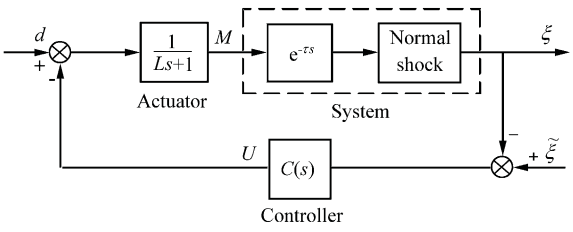

Fig.3 PID regulation system of shock motion.

PID regulator can be described by

$$C(s) = K_p\left(1 + \frac{1}{T_i s} + T_d s\right) \tag{26}$$

When the system meets with an external step disturbance, the proportion controller will work as a main factor at the early time. Therefore, the peak value error C_m is mainly determined by the proportion K_p. Then the value of K_p is obtained by the given peak value error C_m. Thereafter, the phase reserve γ_c is mainly determined by the integral time constant T_i. Because the integral controller will introduce phase delay, derivative controller may be used to increase the phase reserve.

Figs.4-5 show the results for the ith operating point, where the steady error C_∞ equals zero, the peak value error of unit step disturbance C_m 19.2%, and the phase reserve γ_c 53.6°.

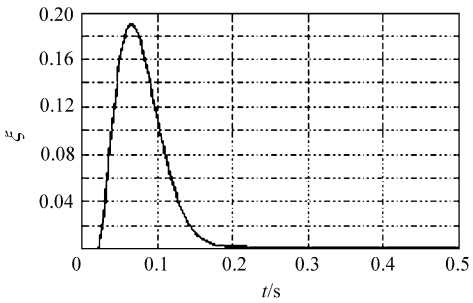

Fig.4 Close-loop response of the system with PID regulator.

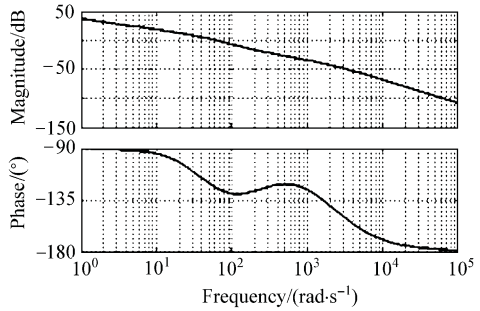

Fig.5 Bode figure of the system with PID regulator.

Different control procedures for different operating points were designed as shown in Table 1 including the design parameters for PID regulator and their corresponding shortcomings. It should be pointed out that there is a contradiction between the peak value error C_m and the bandwidth ω_c. To limit the increase of system's bandwidth, the peak value error must not be too low.

After designing a set of controllers for different operating points, linearly interpolating parameter value method may be used to design the gain scheduling scheme.

Table 1 Table of gain scheduling control

x_s	K_p	T_i	T_d	C_∞	C_m	γ_c/(°)
–0.60	3.3	0.045	0.002	0	0.191	55.2
–0.30	3.2	0.040	0.001	0	0.194	54.7
0	3.0	0.040	0.001	0	0.192	53.6
0.30	3.2	0.040	0.001	0	0.191	56.4
0.60	4.3	0.066	0.004	0	0.187	54.7
0.80	5.0	0.083	0.006	0	0.189	56.8
0.90	5.4	0.100	0.010	0	0.186	54.5
0.95	6.1	0.125	0.012	0	0.189	56.1

Lagrange interpolating parameter value method is used as follows:

$$\left.\begin{aligned} K_p &= \sum_{i=0}^{n}\left[\prod_{j=0,j\neq i}^{n}\frac{x-x_j}{x_i-x_j}\right]K_{pi} \\ T_i &= \sum_{i=0}^{n}\left[\prod_{j=0,j\neq i}^{n}\frac{x-x_j}{x_i-x_j}\right]T_{ii} \\ T_d &= \sum_{i=0}^{n}\left[\prod_{j=0,j\neq i}^{n}\frac{x-x_j}{x_i-x_j}\right]T_{di} \end{aligned}\right\} \quad (27)$$

where the subscripts i and j denote different operating points.

6 Simulation Results

Fig.6 shows the comparison between gain scheduling control and gain fixing control with small disturbance (unit step disturbance), where the difference in peak value errors is only 0.4%. This means that the gain fixing control with small disturbance is valid when a system operates near a certain nominal operating position. Fig.7 shows the comparison between gain scheduling control and gain fixing control with large disturbance (two and a half time the unit step disturbance), where the difference in peak value errors is about 12%. Fig.8 and Fig.9 show the time-dependent changes of control variable U and flue flow rates M with large disturbance respectively.

The results show the merits of gain scheduling control based on the equilibrium manifold linearization model. It should be pointed out that these results were acquired under the assumption of ignoring the influences of upstream conditions. Taking this factor into account in the future, the nonlinearity of the shock motion is anticipated to be strengthened accordingly, and the method proposed in this paper will be more effective.

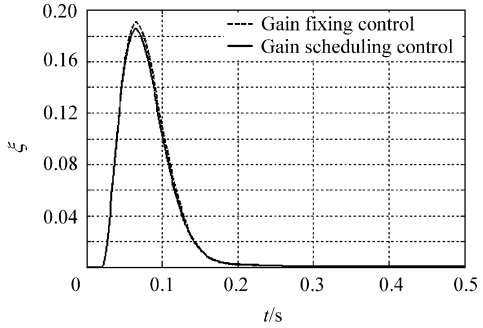

Fig.6 Time-dependent changes of shock position with small disturbance.

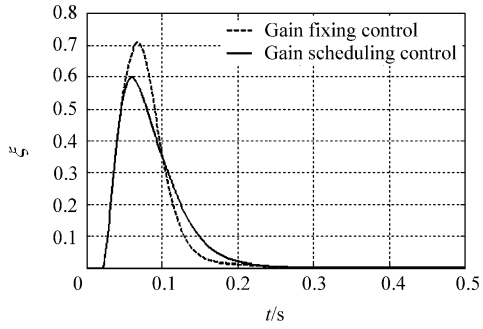

Fig.7 Time-dependent changes of shock position with large disturbance.

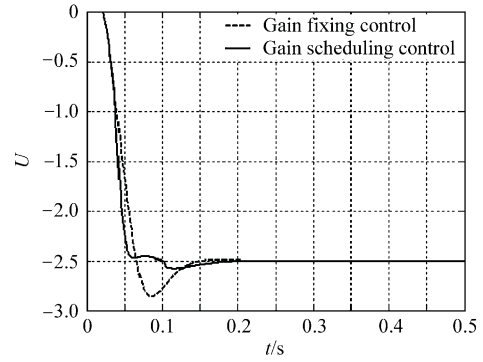

Fig.8 Time-dependent changes of control variable with large disturbance.

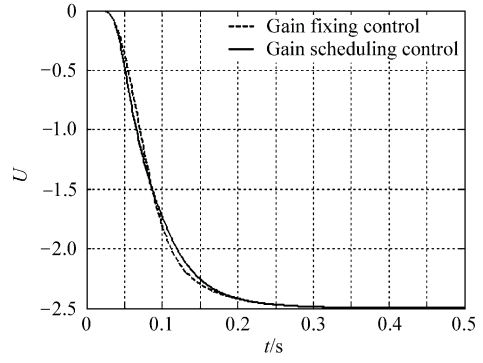

Fig.9 Time-dependent changes of fuel flow rate with large disturbance.

7 Conclusions

The equilibrium manifold linearization model is more accurate than the small perturbation linearization and simpler than the piecewise-linear method. Based on analysis of this model, this paper reveals the self-feedback mechanism of shock motion, which is important for describing the stability and dynamics of shock motion. Also based on this model, the paper designs a gain scheduling control scheme for nonlinear shock motion. Simulation shows the merits of the method when the system suffers from a large disturbance.

References

[1] Susumu M, Keiichi K. Unstart phenomenon due to thermal choke in scramjet module. 10th AIAA/NAL-NASDA-ISAS International Space Planes and Hypersonic Systems and Technologies Conference, AIAA. Kyoto, Japan; 2001.

[2] Mayer D W, Paynter G. C. Prediction of supersonic inlet unstart caused by freestream disturbances. AIAA Journal 1995; 33(2): 266-275.

[3] Xie L R, Guo R W. Numerical simulation and experimental validation of flow in mixed-compression axisymmetric supersonic inlet with fixed-geometry. Chinese Journal of Aeronautics 2007; 28(1): 78-82.

[4] Wang J Q, Ni Z Y. Numerical simulation of two-dimensional super/hypersonic inlet flow fields. Chinese Journal of Aeronautics 2005; 26(2): 153-157.

[5] Yan H, Knight D. Control of normal shock by a single laser pulse. 2th AIAA Flow Control Conference, AIAA. Oregon, 2004.

[6] Salerno M, Malomed B A, Konotop V V. Shock wave dynamics in a discrete nonlinear schrodinger equation with internal losses. Physical Review E—Statistical Physics, Plasmas, Fluids, and Related Inter- disciplinary Topics 2000; 62(6): 8651-8656.

[7] Hurrell H G. Analysis of shock motion in ducts during disturbances in downstream pressure. NACA TN-4090, 1957.

[8] Willoh R G. A mathematics analysis of supersonic inlet dynamic. NASA TND-4969, 1968.

[9] Culick F E, Rogers T. The response of normal shocks in diffusers. AIAA Journal 1983; 21(10): 1382-1390.

[10] Sajben M, Said H. Acoustic-wave/blade-row interactions establish boundary conditions for unsteady inlet flows. Journal of Propulsion and Power 2001; 17(5): 1090-1099.

[11] MacMartin D G. Dynamics and control of shock motion in a near-isentropic inlet. Journal of Aircraft 2004; 41(4): 846-853.

[12] Alonso J S, Burdisso R A. Nonlinear modeling of shock wave trains in ducts with wall discontinuities. 12th AIAA/CEAS Aeroacoustics Conference. Cambridge, MA, United States; 2006.

[13] Yu D R, Cui T, Bao W. Equilibrium manifold linearization model for normal shock position control systems. Journal of Aircraft 2005; 42(5): 1344-1347.